

## Non destructive electrical defect characterisation and topography of silicon wafers and epitaxial layers

K. Dornich, T. Hahn, and J.R. Niklas

Technische Universität Bergakademie Freiberg, Silbermannstr.1, D-09596 Freiberg, Germany  
corresponding author: Electronic address: KayDornich@gmx.de

### Abstract

Recent progress in experimental technique made it possible to improve the sensitivity of microwave detected photoconductivity by several orders of magnitude. This opens completely new possibilities for a contact less non-destructive electrical defect characterization of silicon wafers and even of epitaxial layers on substrates with extremely low resistivity. Electrical properties such as lifetime, mobility and diffusion length can be measured without contacts also at very low injection levels with a resolution only limited by the diffusion length of the charge carriers. The doping level of the material plays no major role.

Owing to the high sensitivity, thermal excitation of charge carriers out of defect levels filled during the photo pulse can also be observed. This leads to defect specific photoconductivity transients which deliver pieces of information like DLTS, however, again without contacts, non critical doping, and with high spatial resolution.

### Experimental procedure

Absorption of light inducing band-to-band transitions generates excess charge carriers giving rise to a photoconductivity signal. However, rather than to measure the photoconductivity by contacts the excess carriers are detected by microwave absorption. Using a laser generating a very small light spot on the wafer, the experiments can be carried out with high spatial resolution. A typical response to a rectangular light pulse is shown in Fig. 1. The rapid decay after switching off the light is due to recombination of free carriers (lifetime  $\tau$ ). With the light on, carriers are also trapped by different defect levels. These carriers are thermally re-emitted with the light pulse off giving rise to a sometimes extremely small slow transient referred to as "defect part" in Fig. 1. This defect part furnishes valuable information about electrical properties of the defect as will be shown later. The light pulse must be long enough in order to fill all defect levels of interest. Once a defect level is filled, the re-emission signal (defect part) does definitely not depend on the light intensity. It is proportional to the defect concentration. In order to detect the defect part of the transient signal also at low defect concentrations it is therefore necessary to keep the light intensity sufficiently low not to overload the detection system by a too high photo pulse signal. Presently commercially available systems fail in the detection of the defect part due to a sensitivity some orders of magnitude too low. The effect of light intensity (injection level) on the amount of the defect signal is illustrated in Fig. 2.

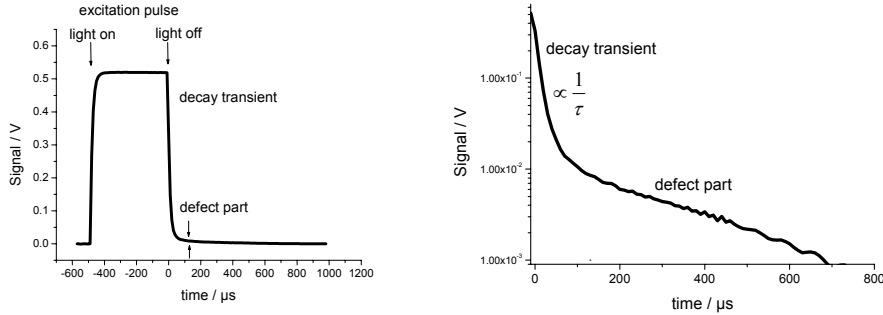


**Figure 1:** Left part: Photoconductivity signal for a rectangular light pulse, p silicon wafer.  
Right part: The transients due to recombination of free carriers and re-emission from defect levels, respectively, are clearly to be seen from the log plot

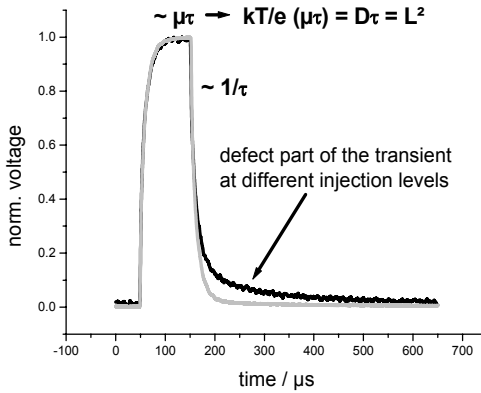


**Figure 2:** Amount of defect signal part relative to the photo pulse signal for the same defect at two different injection levels. The photo pulses are normalized. The higher amount of defect signal in the figure corresponds to a lower injection level. P silicon sample, further details see text

In Fig. 2 there it is also illustrated what pieces of information can be deducted from different parts of the signal and the transients. At constant laser excitation, the photo pulse intensity is proportional to the carrier mobility,  $\mu$ , times the carrier lifetime,  $\tau$ . Using Einstein's relation for the carrier diffusion constant,  $D$ , it becomes evident that the photo pulse intensity is proportional to the square of the diffusion length,  $L$ . The lifetime,  $\tau$ , can be measured independently by the rapid decay transient of the photo pulse. Thus it is finally possible to obtain  $L$  or  $\tau$  topograms, respectively. The spatial resolution is geometrically determined by the diameter of the laser light spot.  $10\mu\text{m}$  is a typical value, but  $1\mu\text{m}$  might be also possible. However, the actual achievable spatial resolution is finally limited by the diffusion length of the free carriers, which e.g. for typical silicon wafers may considerably exceed  $10\mu\text{m}$ .

There is one further very important point: As it is well known from the Shockley-Read-Hall relation, the free carrier lifetime,  $\tau$ , depends severely on the concentration of these carriers and thus on the injection level. It is therefore a question of what value for  $\tau$  one wants to measure to decide what injection level is necessary in order to actually get this value. It seems obvious, that in order to somehow predict the properties of devices when measuring properties of the starting wafer material one should aim at injection levels during the measurement which are typical for the normal function of the devices in mind. E.g., for solar cells, this level is about  $100\text{mW/cm}^2$

("one sun"). At these levels, e.g.  $\tau$ - topograms look extremely different from those obtained at injection levels up to four orders of magnitude higher as used by presently commercially available systems due to sensitivity problems. None of the effects shown in the following are seen at these high levels. We termed the measurement technique capable of obtaining L- or  $\tau$ - topograms measured contact less by microwave absorption at injection levels down to at least  $100\text{mW/cm}^2$  with laser spot diameters small compared to the diffusion length "microwave detected photoconductivity" (MDP).

A closer inspection of the so- called defect part of the photoconductivity transients as discussed e.g. in Fig. 2 opens completely new ways for a topographic contact less analysis of electrical defect properties. In fact, evaluating the defect transients as in Fig.2 exactly in the same way as one usually does with DLTS capacitance transients delivers similar information about the defect as DLTS does. Those pieces of information are activation energy of the defect, cross sections for the interactions with electrons or holes, and an estimation of defect concentration. It is even possible to measure DLTS- like defect spectra this way by measuring and evaluating the defect transients (Fig.2) as a function of temperature. Examples are shown below. We termed the new technique "microwave- detected photo induced current transient spectroscopy" (MD-PICTS). It is beyond the scope of this short introduction to go further into the details of the features of MD-PICTS versus DLTS. This will be treated in forthcoming more specific papers. Some more aspects of MD-PICTS are already found in the literature [1,2].

The measurement system for MDP and MD-PICTS is depicted in Fig. 3. Absorption (not reflection) of a microwave electromagnetic field of about 10GHz is used to measure the photo conductivity of the sample. For mappings, transients are measured while the wafer is moved in the x-y-plane. The spatial resolution is determined by the size of the laser spot, however, in most practical cases by the considerably longer diffusion length of the free carriers.

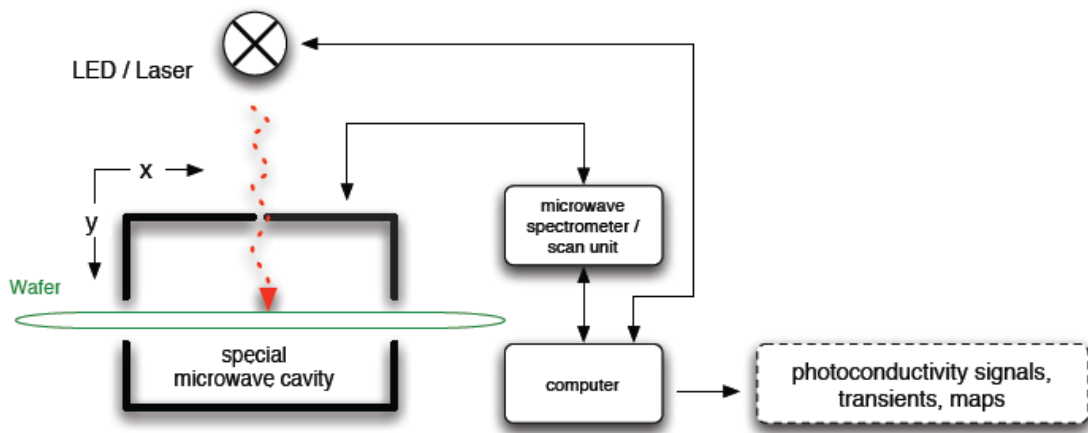


**Figure 3:** MD – PICTS/ MDP measurement system, details see text.

The sample or wafer is electrically part of a special microwave system. Key feature is the appropriate coupling of the sample to the resonant microwave cavity. The apparatus allows for a free movement of e.g. wafers of principally unlimited size. For MD-PICTS, the wafer must be part of a cryostat system which provides a further experimental challenge. The injection levels used correspond to an optical power of the light source in the range of about  $10\mu\text{W}$  to  $10\text{mW}$  depending on the defect concentration and type of semiconductor. In MD-PICTS, the lowest power levels are essential for the investigation of the lowest defect concentrations. It is very

difficult to give an estimate about the lowest detectable defect concentration. This depends in the first place on the DC- conductivity of the sample and on the spatial resolution desired. Details are still under investigation. In favourable cases, MD-PICTS defect spectra could be measured on high purity silicon wafers with defect concentrations below the detection limit of DLTS. In some cases the detection limit for metal contaminants is below  $10^{10} \text{ cm}^{-3}$ , however the ultimate detection level is not yet explored and depends on the material and the kind of defect. If spatial resolution is not a prime concern, the laser may be replaced as well by a light emitting diode. Some depth information of defect distributions can be achieved by using light of different wavelengths and hence different penetration depths [3,4].

## Experimental results

MDP and MD-PICTS can be applied to a wide variety of semi conducting and even insulating materials, in particular, silicon materials ranging from polycrystalline, electronic grade material to even thin epitaxial layers. It turned out that completely new features are seen in the MDP-maps. Very fine crystal growth imperfections and damages due to surface preparation, polishing, and handling along with the wafer fabrication are also seen in great detail, even for the highest quality silicon wafers. The applicability of MDP and MD-PICTS is independent of the doping level. The resistivity of the sample can be as low as about  $0.1\Omega\text{cm}$ , there is no upper limit. The investigation of epitaxial layers on extremely low resistivity substrates (about  $10\text{m}\Omega\text{cm}$ ) provides the greatest challenge for the applicability of the new techniques. Even this is now feasible. As an example, Fig. 4(a) shows the diffusion length contrast of an layer. Fig. 4(b) shows the photoconductivity responses at two different locations as indicated by the arrows. The inhomogeneity of the lifetime is clearly to be seen. The laser wavelength is 657nm.

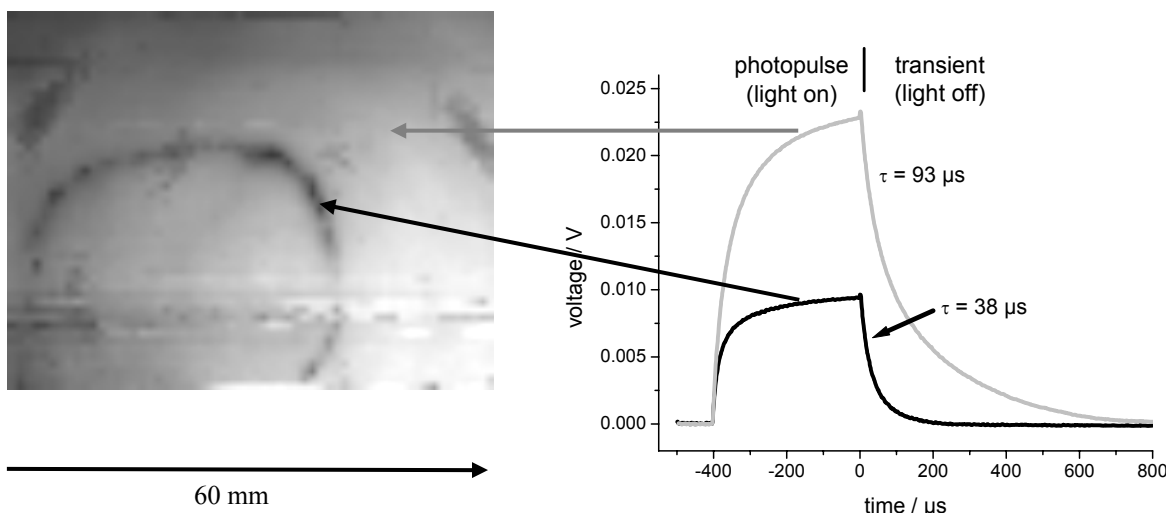


**Figure 4:** Diffusion length map of an passivated EPI layer n/n+, EPI:  $15 \Omega\text{cm}$ ,  $50 \mu\text{m}$ ; Substrate:  $0.02\Omega\text{cm}$  (a), corresponding photoconductivity transients at two different locations (b)

Fig. 5(a) shows the same epitaxial wafer as in Fig. 4, however, measured without surface passivation. Surface recombination dominates (Fig. 5a). Using a 975 nm laser generates excess carriers also at the backside of the EPI layer ( $60 \mu\text{m}$  penetration depth). As a consequence, Fig. 5b now shows the recombination behavior at the substrate / EPI layer interface with lifetime

inhomogeneities of about 20%. Investigating the layer with 657 nm laser light which penetrates only by about 3  $\mu\text{m}$  into the layer results in information about the recombination within the EPI layer itself since the surface is passivated (Fig.5c).

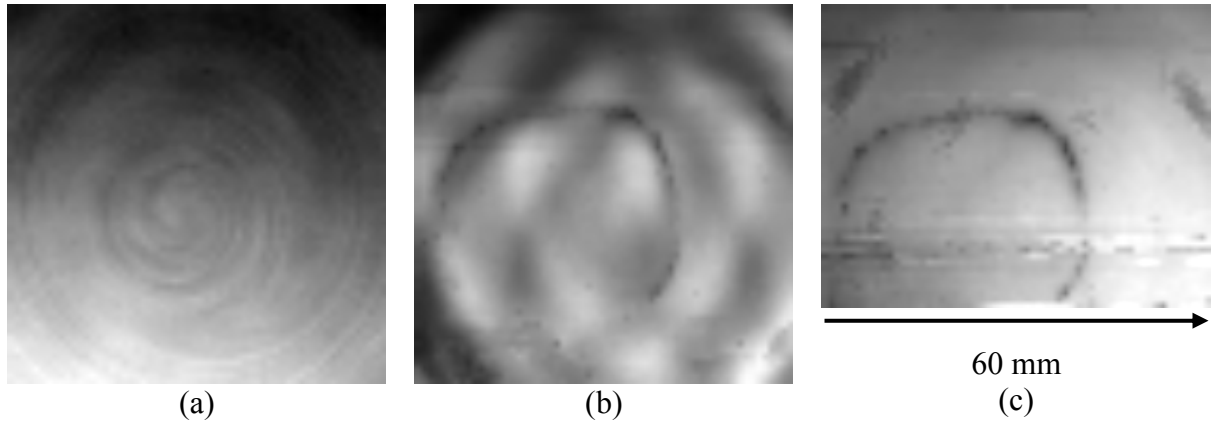


**Figure 5:** Diffusion length maps: not passivated EPI at 975 nm (a), passivated EPI at 975 nm (b), passivated EPI at 657 nm (c)

It follows from these results that the diffusion length of the minority carriers (holes) in the EPI layer must be considerably smaller than 50  $\mu\text{m}$ .

As just one example for a defect characterization by MD-PICTS Fig. 6 shows a defect spectrum for a p Czochralski grown silicon wafer for different heat treatments. Note again that the measurements take place without contacts and that they are spatially resolved. Peak one corresponds to the well known thermal donor [5]. This peak cannot be detected by DLTS in p silicon. The black curve shows an as-grown sample with an activation energy for peak one of about  $E_A = 0.13\text{ eV}$  and a capture cross section  $\sigma = 1.9 \cdot 10^{-18}\text{ cm}^2$ .

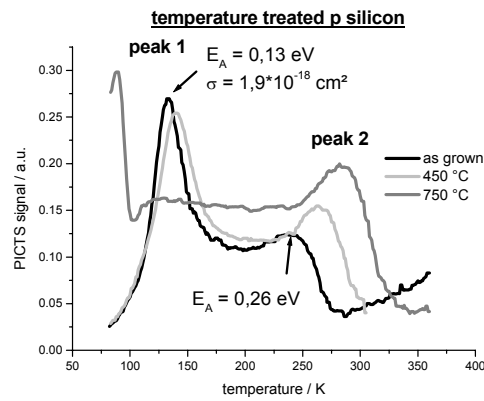


**Figure 6:** MD – PICTS defect spectra for a p Czochralski grown silicon wafer for different heat treatments

Peak two exhibits an activation energy of 0.26 eV. After 450°C heat treatment peak one shifts slightly to higher temperatures and peak two shifts to  $E_A = 0.37\text{ eV}$ . After 750°C annealing, peak one moves almost 50°C to lower temperatures. This is explained by a conversion of the thermal

donor from an electrically active centre into an electrically inactive trap centre. The defect corresponding to peak two is not yet well known. Flat lines in the MD-PICTS spectra are due to constant defect emission from most likely shallow trap states over a certain temperature range, this can be shown by variation of the sample type or crystal growth conditions.

## Conclusion

The new measurement techniques of MDP and MD-PICTS provide completely new so far not available facilities for a non-destructive spatially resolved electrical characterisation and investigation of semiconducting materials, in particular silicon. It should be stressed, that e.g. the measurements of minority carrier lifetimes can take place at injection levels which are realistic for devices. This for example reveals the relevance of so far not seen recombination centres and gives new hints for an optimisation of materials and processing steps. Since the methods are non-destructive they are ideally suited for an integration into production lines and for process monitoring. They provide for the first time non-destructive access to device relevant electrical parameters of epitaxial layers. There are many new applications one can think of, like the investigation of SiGe and SOI layers and e.g. problems of wafer bonding, or the investigation of electrical parameters and defects in completely new materials. So far we just tried besides electronic grade silicon mc-Si, GaAs, InP, SiC, Ge and CGS [6-8].

## Acknowledgements

Financial support and delivery of samples by the companies Freiberg Compound Materials (FCM), Siltronic AG, Solar World AG, and Z-Foundry (ZMD AG) are gratefully acknowledged.

## Literature

1. Gründig-Wendrock, B., Jurisch, M., Niklas, J.R., Materials Science and Engineering B91-92, 371-375, (2002)
2. J.R. Niklas, W. Siegel, M. Jurisch, U. Kretzer, Mat. Science and Engin. B80, 206-209, (2001)
3. K. Dornich, B. Gründig-Wendrock, T. Hahn, J.R. Niklas, Advanced Engineering Materials, 598-602, (2004)
4. K. Dornich, T. Hahn, J.R. Niklas, Freiberger Forschungshefte B327, 270 – 278, (2004)
5. A. Borghesi, B. Pivac, A. Sassella, A. Stella, J. Appl. Phys. 77 (9), 4169 – 4244, (1995)
6. A. Wohlrab, B. Gruendig - Wendrock, M. Jurisch, F.-M. Kiessling and J.R. Niklas, Eur. Phys. J. Appl. Phys., Vol. 27, No. 1-3, 223-226, (2004)
7. B. Gruendig - Wendrock and J.R. Niklas, Phys.stat.sol., No. 3, 885-888, (2003)
8. B. Gruendig - Wendrock, K. Dornich, T.Hahn, U. Kretzer and J.R. Niklas, Eur. Phys. J. Appl. Phys., Vol. 27, No. 1-3, 363-366, (2004)